Surface Stresses of Thick Concrete Pavement Slabs Due To Traffic Loads and Non-Linear Temperature Distributions.

Tatsuo Nishizawa[1], Takato Ozeki[2], and Hirotaka Kawano[3]

Abstract
In this study, possibility of top-down cracking in concrete pavement was investigated. The main cause of the crack is supposed to be tensile stress at the top of the concrete slab. 3DFEM simulations that took into account actual temperature distributions throughout slab depth were performed on concrete pavements for a heavy duty road and an international airport. Thermal stress analysis revealed that nonlinear negative temperature distribution produces relatively large tensile stress at the top of the slab, which cannot be precisely estimated by conventional thermal stress equations based on the linear temperature distribution. Areas where the bottom surface of concrete slab was separated from the surface of underlying layer were very small, because the underlying layer deformed similarly as the slabs deformed and reduced the gap area. The combined stresses were also calculated with the application of both wheel and thermal loads. The maximum top combined stress occurred at a position away from the wheel loads. The ratio of the top combined stress in negative temperature gradient to the bottom combined stress in positive temperature gradient is greater in the airport pavement than that in the road pavement. The installation of dowels in joints reduced the combined stress in the loaded slab.

Introduction

One of the primary distress modes in concrete pavement is cracking in concrete slabs. Cracks that are produced by wheel load and/or thermal load should be considered in the structural design of concrete pavement. The direct cause of the crack is supposed to be tensile stress repetition at the bottom of the slab due to wheel load and temperature distribution throughout slab depth. The maximum bottom stress occurs just under a wheel load in positive temperature gradient condition (temperature at the top of the slab is higher than that at the bottom). In the current Japanese design, the combined stress that is an addition of wheel stress and thermal stress is calculated and applied to a fatigue curve to estimate the fatigue damage (Iwama 1963). In the design, it is assumed that the maximum combined stress occurs at the bottom of the concrete slab and induces bottom-up crack at the midslab. In USA, on the other hand, top-down cracks that are caused by tensile stress at the top of the slab are considered as a critical distress (ARA, Inc. 2004). The maximum top stress occurs at a position between steering axle and driving axles in negative temperature gradient condition. Similar situation takes place in concrete slab with build-in curling that is created by contraction differential between the top and bottom of the slab in early stage of construction (Hiller and Roesler 2006). Full scale tests conducted on concrete pavements in FAA National Airport Pavement Test Facility also showed that top-down cracking was rather dominant distress mode of concrete slab (Guo 2006). In

[1]Professor, Ishikawa National College of Technology. Address: Tsubata, Ishikawa, 929-0392, Japan. E-mail: nishi@ishikawa-nct.ac.jp
[2]Engineer, Taisei Construction Company. Address: 1-25-1Nishi-Shinjyuku, Shinjyuku-ku, Tokyo, 160-0606, Japan. E-mail: ozktkt00@pub.taisei.co.jp
[3]Professor, Kyoto University. Address: Katsura, Kyoto University, Nishikyo-ku, Kyoto, 615-8540, Japan.

Japanese roadways, longer concrete slabs (8 to 10m) are adopted to reduce the number of joints, which would increase the risk of top-down cracking. The same thing can be said for airport concrete pavement, because thick and large size slabs (8m by 8m) are used.

It has been recognized that temperature distribution through slab depth exhibits strong nonlinearity in thick concrete slab and the non-linearity significantly affects the thermal stress (Choubane and Tia 1995, Pane et al. 1998, Shoukry et al. 2003, Mahboub et el. 2004). The thermal stress calculated with an equation that uses the temperature differential is quite different from the actual thermal stress because of non-linear component. That makes the bottom tensile stress overestimated, while it makes top tensile stress underestimated. Therefore, the nonlinearity in the negative temperature gradient increases the risk of top-down cracking.

In this study, the effect of non-linearity of temperature distribution throughout slab depth on the top tensile stress was investigated. The combined stresses due to wheel and thermal loads were calculated in the actual wheel load and temperature conditions for concrete pavements for a road and an airport. Comparisons on the top tensile stresses between linear and nonlinear temperature distributions was made to discuss the possibility of top-down cracking in the concrete pavements. Also, the effectiveness of dowel reinforcement at joints to reduce the stresses was examined.

3DFEM Analysis of Thermal Stress

Three dimensional finite element method (3DFEM) was employed in this study to calculate thermal and/or wheel load stresses, because the method is able to simulate thermal behaviors of concrete slabs as well as the underlying layers accounting for mechanical interactions between them (Nishizawa et al. 2005). Also, it is able to directly take into account the nonlinear temperature distribution throughout slab depth.

Formulation of thermal stress. Thermal stress can be calculated by

$$\{\sigma\} = [\mathbf{D}](\{\varepsilon\} - \{\varepsilon_T\}) = [\mathbf{D}]\{\varepsilon_R\} \qquad (1)$$

Where,

$\{\sigma\}$ = stress vector,

$[\mathbf{D}]$ = elastic matrix,

$\{\varepsilon\}$ = total strain vector,

$\{\varepsilon_T\}$ = thermal strain vector, and

$\{\varepsilon_R\} = \{\varepsilon\} - \{\varepsilon_T\}$ = restrained strain vector.

In the three dimensional space, the thermal strain is:

$$\{\varepsilon_T\} = \{\alpha T \quad \alpha T \quad \alpha T \quad 0 \ \ 0 \ \ 0\} \qquad (2)$$

Where, T is the temperature and is assumed to be a quadratic function of z as proposed by the authors (Nishizawa et al. 2005). The stiffness equation of FEM with thermal stress becomes:

$$[[\mathbf{K}] + [\mathbf{J}]]\{\mathbf{d}\} = \{\mathbf{f}_w\} + \{\mathbf{f}_p\} + \{\mathbf{f}_t\} \qquad (3)$$

Where,

$[\mathbf{K}]$ = stiffness matrix for concrete slab, base courses and subgrade,

$[\mathbf{J}]$ = joints and interface between the concrete slab and base course,

$\{\mathbf{d}\}$ = displacement vector,

$\{\mathbf{f}_w\}$ = self-weight load vector,

$\{\mathbf{f}_p\}$ = external load vector,

$\{\mathbf{f}_t\} = \int_V [\mathbf{B}][\mathbf{D}]\{\varepsilon_t\}dV$: thermal load vector and

$[\mathbf{B}]$ = displacement-strain matrix.

When a concrete slab is lift off by a temperature gradient, parts of the slab bottom surface are separated from underlying layer. This can be modeled by setting very week vertical spring of the interface element in the separated parts. This method makes Eq.(3) nonlinear, because $[\mathbf{J}]$ in Eq.(3) changes according to $\{\mathbf{d}\}$. To solve the non-linear equation, a combination of the Newton-Raphson method and the load incremental method was employed. A 3DFEM program, Pave3D, was developed using the formulation and used to calculate combined stresses in the concrete slab due to wheel and thermal loads (Nishizawa et al. 2009).

3DFEM model. In this study, two pavement structures were assumed for investigation. One was for a heavy duty road with two lanes and the other was for an international airport. 3DFEM model of the concrete pavement for the road is shown in Figure 1. The road pavement had 300 mm thick concrete slabs on a 40 mm thick asphalt interlayer and a 150 mm thick granular base course. Dowel bars with a diameter of 32 mm and a length of 700mm were installed with a spacing of 400 mm in the transverse joint, and tie bars with a diameter of 25 mm and a length of 1000 mm were installed with a spacing of 1000 mm in the longitudinal joint. Wheel loads of a tandem rear axle with a magnitude of 24.5 kN per wheel were applied at the jointed corner of a slab.

The airport pavement had a 460 mm thick concrete slab with a size of 8 m by 8m. Twelve of the slabs were connected with doweled joints and placed on an 120 mm thick asphalt interlayer and a 230 mm granular base course. Dowel bars with a diameter of 42 mm and a length of 700 mm were installed with a spacing of 400 mm. Four gear loads of B-747-400 with a magnitude of 230 kN per wheel were applied as shown in Figure 2, where a gear load was located at a jointed corner.

These load locations were selected because the corner loading is expected to produce large tensile stress on the top of the slabs. Load transfer across the joints was provided by the dowel bars, which was modeled with a special interface element developed by the author (Nishizawa et al. 2005).

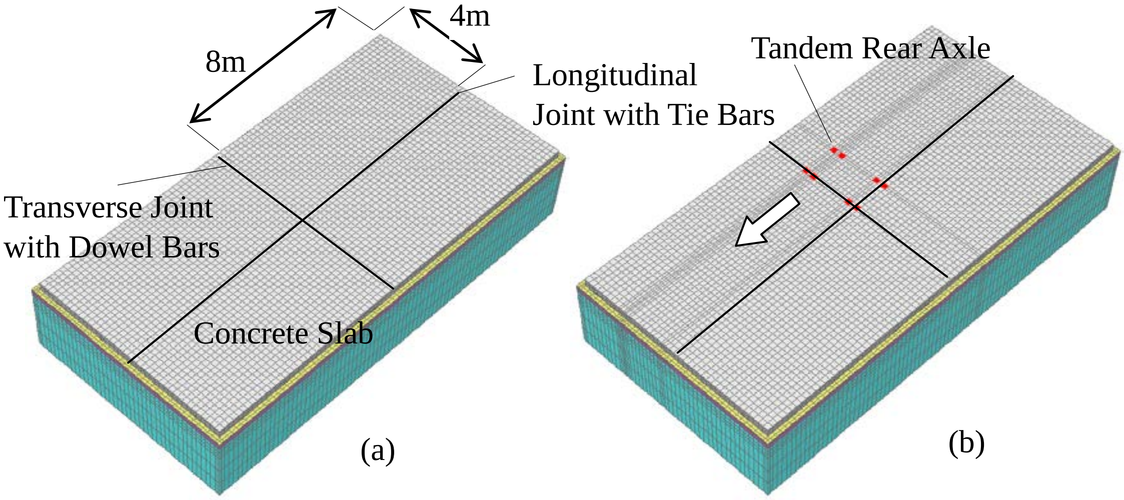

Figure 1. 3DFEM modeling of concrete pavement for a heavy duty road: (a) thermal loading and (b) wheel loading

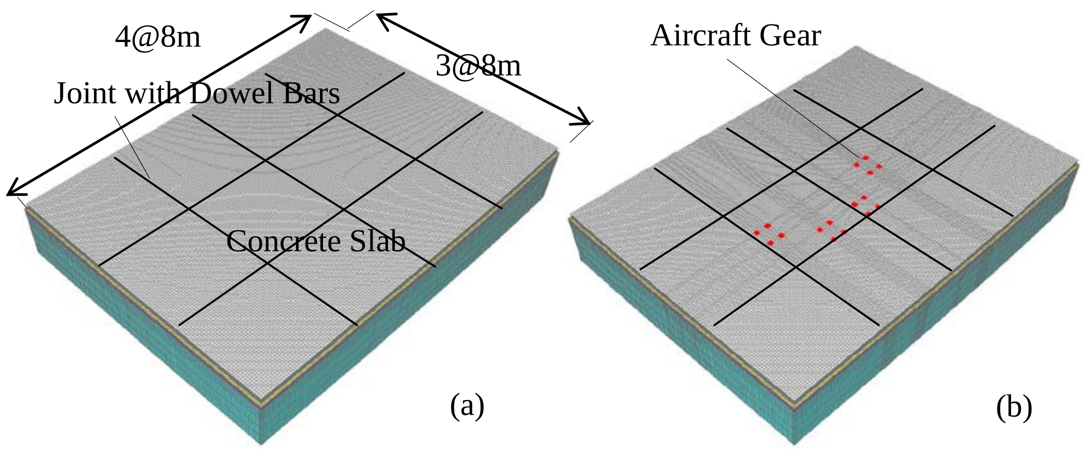

Figure 2. 3DFEM modeling for an international airport:
(a) overview and (b) wheel loading condition.

Table 1 presents material properties used in this study, whose values were selected as a typical one for each material used in Japanese design. The mechanical interaction between the concrete slabs and asphalt interlayer was modeled by the interface element with two horizontal springs and one vertical spring. The value of the horizontal spring constant was small to allow a horizontal slip movement and eliminate the horizontal constraint to temperature volume change of the concrete slabs. The value of the vertical spring constant was changed depending on displacements at the interface to model the separation as mentioned earlier.

Table 1. Input parameters of material properties in 3DFEM analysis.

Concrete Slab		
Thickness[mm]	300	460
Elastic Modulus [MPa]	29400	
Poisson's Ratio	0.2	
Density[g/cm^3]	0.0023	
Thermal Expansion Coefficient [/^{o}C]	$10 * 10^{-6}$	
Interface between Slab and Asphalt Interlayer		
Horizontal Spring Constant [MN/m^3]	1.0	
Vertical Spring Constant [MN/m^3]	$10 * 10^6$ or 1.0	
Asphalt Interlayer		
Thickness [mm]	40	120
Elastic Modulus [MPa]	1960	
Poisson's Ratio	0.35	
Granular Base Course		
Thickness [mm]	150	320
Elastic Modulus [MPa]	490	
Poisson's Ratio	0.35	
Subgrade		
Thickness [mm]	2500	4000
Elastic Modulus [MPa]	78.4	
Poisson's Ratio	0.35	

Thermal Load. For the thermal load, temperature distributions throughout slab depth as shown in Figure 3 were applied to the slab. They were calculated by solving one dimensional heat transfer equation with surface boundary temperatures measured at a concrete surface at 3:00 on Aug. 12 for the negative temperature gradient and 13:00 on Aug. 12 for the positive one (Nishizawa et al 2009). Since Pave3D is able to account for linear and non-linear temperature distributions, both temperature distributions were used to find the difference in thermal stresse. In case of liner temperature distribution of 300 mm thick concrete slab, the temperature gradients were -0.018 ^{o}C/mm for the negative gradient and 0.033 ^{o}C/mm for the positive one. In 460 mm thick slab, they were -0.012 ^{o}C/mm and +0.024 ^{o}C/mm, respectively.

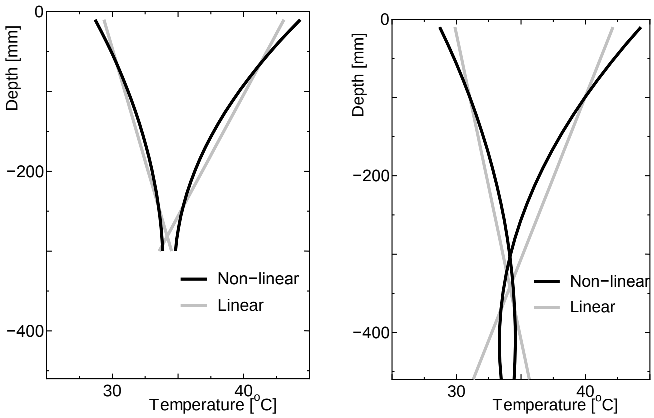

Figure 3. Temperature distributions assumed in 3DFEM analysis.

Thermal Stress Analysis.

To look into the fundamental characteristics of thermal stress, only thermal load was applied and responses of the concrete pavements were calculated with the Pave3D program.

Entire Slab Responses to Thermal Load. Figure 4a shows a curling deformation of the pavement due to the negative temperature gradient. In this Figure, two concrete slabs are not displayed to show the deformation of the underlying layer. All corners of the slabs curl up and the underlying layer similarly deforms. Therefore, the separation area of the slab from the underlying layer is limited in a 0.2 m band from the joint edge. Figure 4b shows the maximum principal stresses on the top of the slabs. Large tensile stresses appear in a wide area of the middle part of the slab. The maximum tensile stress occurs at the center of the longitudinal edge of the slab.

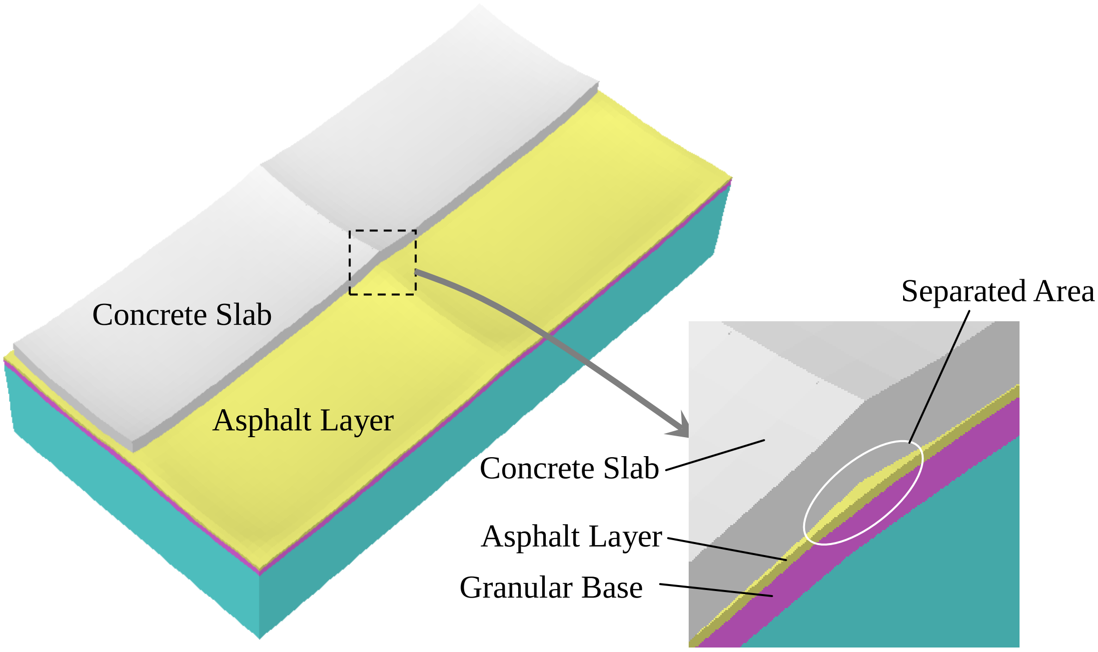

(a)

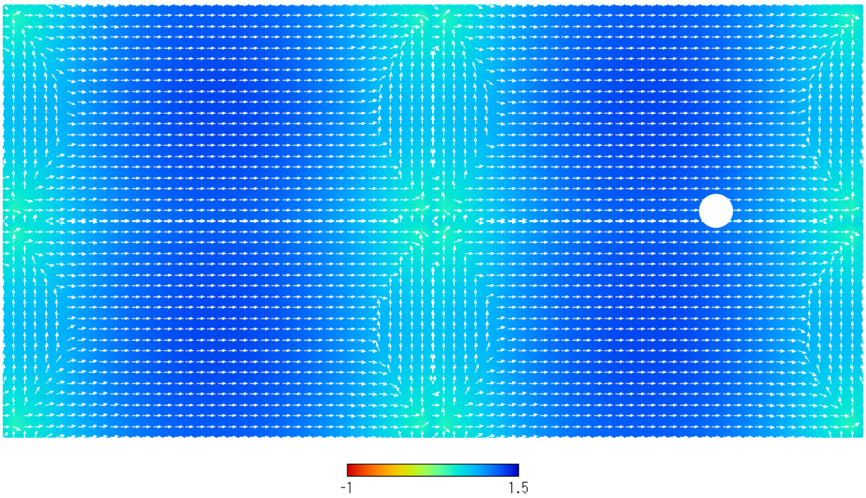

(b)

Figure 4. Entire responses of the road pavement: (a) curling deformation due to negative thermal load, (b) contour and directions of the top maximum principal stress. White circle indicates the position of the maximum tensile stress.

Figure 5 shows similar responses of the airport pavement. A curling deformation is shown in Figure 5a, where a portion of the slabs is not displayed to show the deformation of the underlying layer. All slabs curl up at their corners. Separation between the slab and the underlying layer appears in very small areas at the slab edge, because the doweled joints constrain the curling movement and the underlying layer deforms as the concrete slabs do. Figure 5b shows the contour of the top stress and vectors of two loaded slabs. Again, the top principal stresses are tensile in a large part of the surface and their directions are parallel to the direction of the slab edge. The maximum tensile stress occurs at the center of the slab.

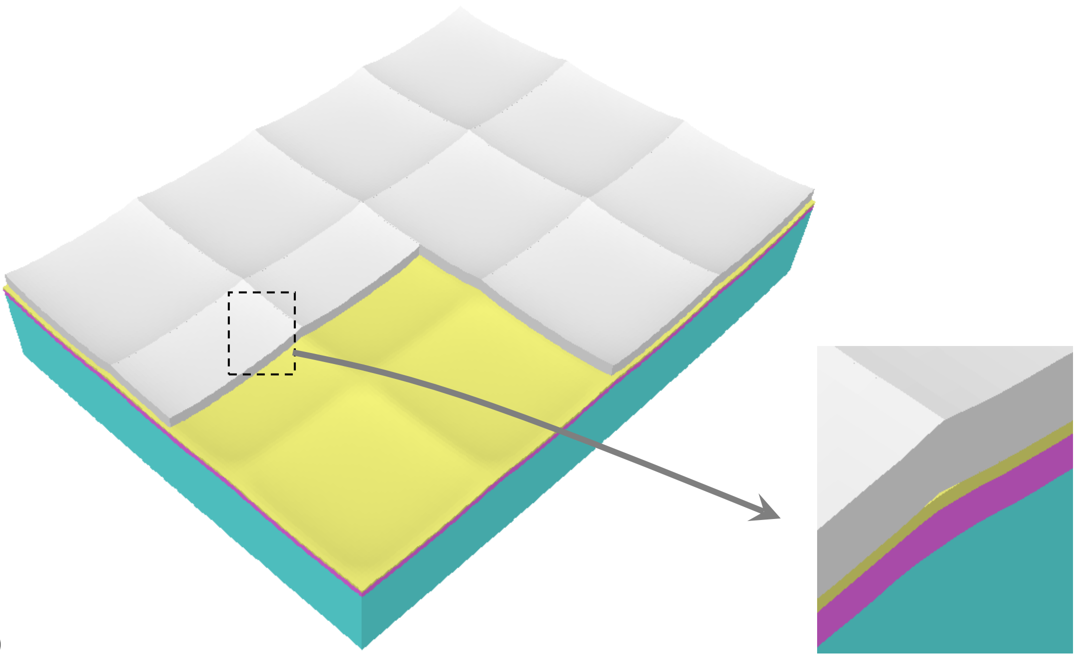

(a)

(b)

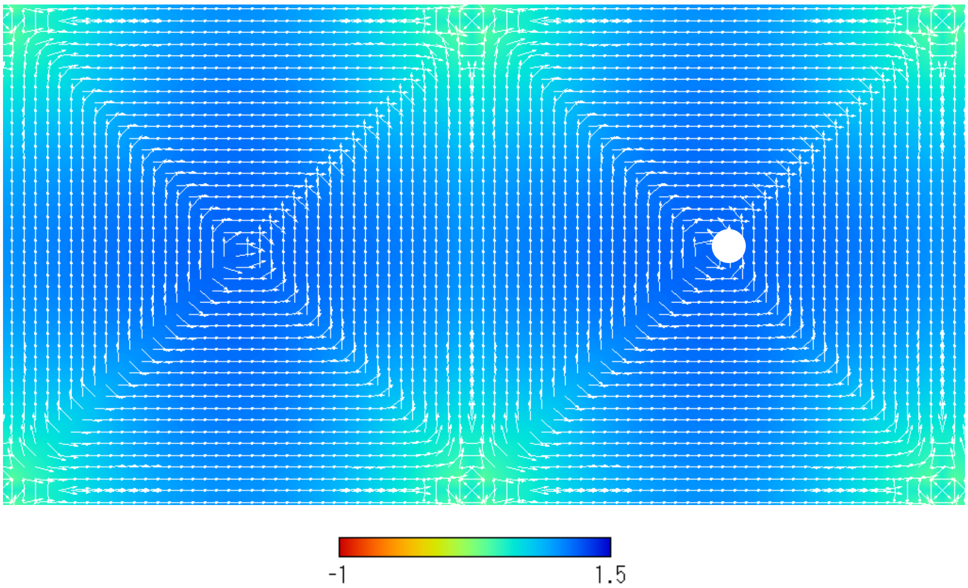

Figure 5. Entire responses of the airport concrete pavement:
(a) curling deformation due to negative thermal load, (b) contour and directions of top maximum principal stress. White circle indicates the position of the maximum tensile stress.
(b)

The Maximum Thermal Stress. Figure 6 shows thermal stress distributions throughout the slab depth at the center of the slab for both negative and positive temperature gradients. In the positive temperature gradient, tensile stress occurs at the bottom of slab. The non-linear thermal stress generated by the non-linear temperature distribution, is smaller at the bottom and larger at the top than the linear thermal stresses generated by the linear temperature distribution. In the negative temperature gradient, the situation is the same except that the sign of stress is the opposite. Thus, the conventional thermal stress equations based on the linear temperature distribution would underestimate the top thermal stress.

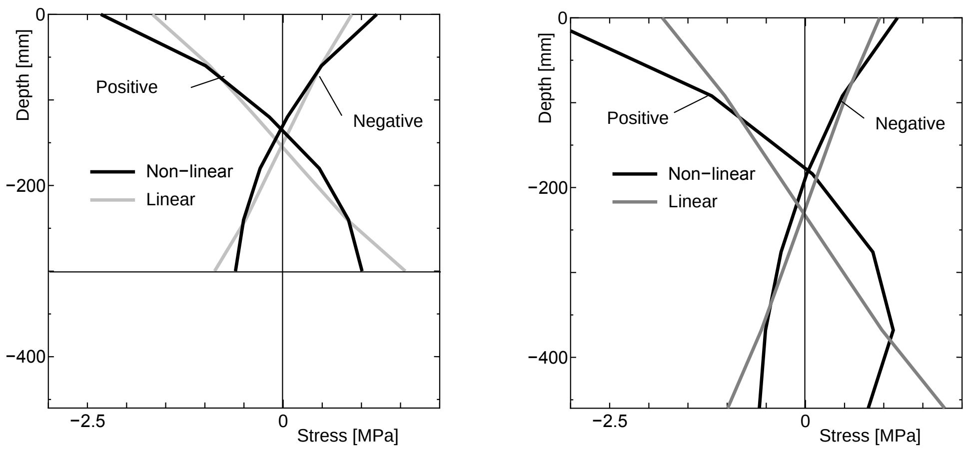

(a) (b)

Figure 6. Thermal stress distributions throughout slab depth in (a) 300 mm thick slab and (b) 460mm thick slab.

Table 2 compares the magnitude of the linear and nonlinear thermal stresses at the center of the slab. The ratio of the nonlinear stress to the linear stress is presented in the table. In the 300mm thick slab, the nonlinear stresses are more than 30 % larger than the linear stress at the top of the slab, while at the bottom of the slab they are about 30 % less. This can be said for both negative and positive temperature gradients. In the 460 mm thick slab, the nonlinear tensile stress is 24 % larger than the linear one at the top of the slab in the negative temperature gradient. In the positive temperature gradient, the nonlinear tensile stress is about a half of the linear one.

Table 2. Comparisons of the linear and nonlinear thermal stresses (MPa).

300mm						
Temperature Gradient	Positive Gradient			Negative Gradient		
	Linear	Non-Linear	Ratio(N/L)	Linear	Non-Linear	Ratio(N/L)
Top	-1.804	-2.489	1.380	0.945	1.275	1.350
Bottom	1.743	1.167	0.670	-0.956	-0.681	0.712
460mm						
Temperature Gradient	Positive Gradient			Negative Gradient		
	Linear	Non-Linear	Ratio(N/L)	Linear	Non-Linear	Ratio(N/L)
Top	-1.827	-3.362	1.840	0.949	1.176	1.239
Bottom	1.779	0.803	0.451	-0.993	-0.588	0.592

Combined Stress Analysis

In order to simulate actual situations of the concrete pavements, combined stresses due to the wheel and negative thermal loads were calculated.

Entire Slab Responses to Wheel and Thermal Loads. Figure 7 shows the entire responses of the road pavement to the wheel and thermal loads. Since the pavement has doweled transverse joint and tie-bared longitudinal joint, not only the corner of loaded slab but also the corners of unloaded slabs deform downward as shown in Figure 7a. A small separation is observed only at the unladed slab edge. The other corners remain curling up. Figure 7b shows a contour and vectors of the maximum principle stress on the top of the slab. The top stress in the loaded area decreases from that of thermal load because the wheel load stress is compressive on the top of the slab. The stress state away from the wheel loads is almost the same as that of thermal load. The maximum tensile stress occurs at the position marked with a white circle in Figure 7.

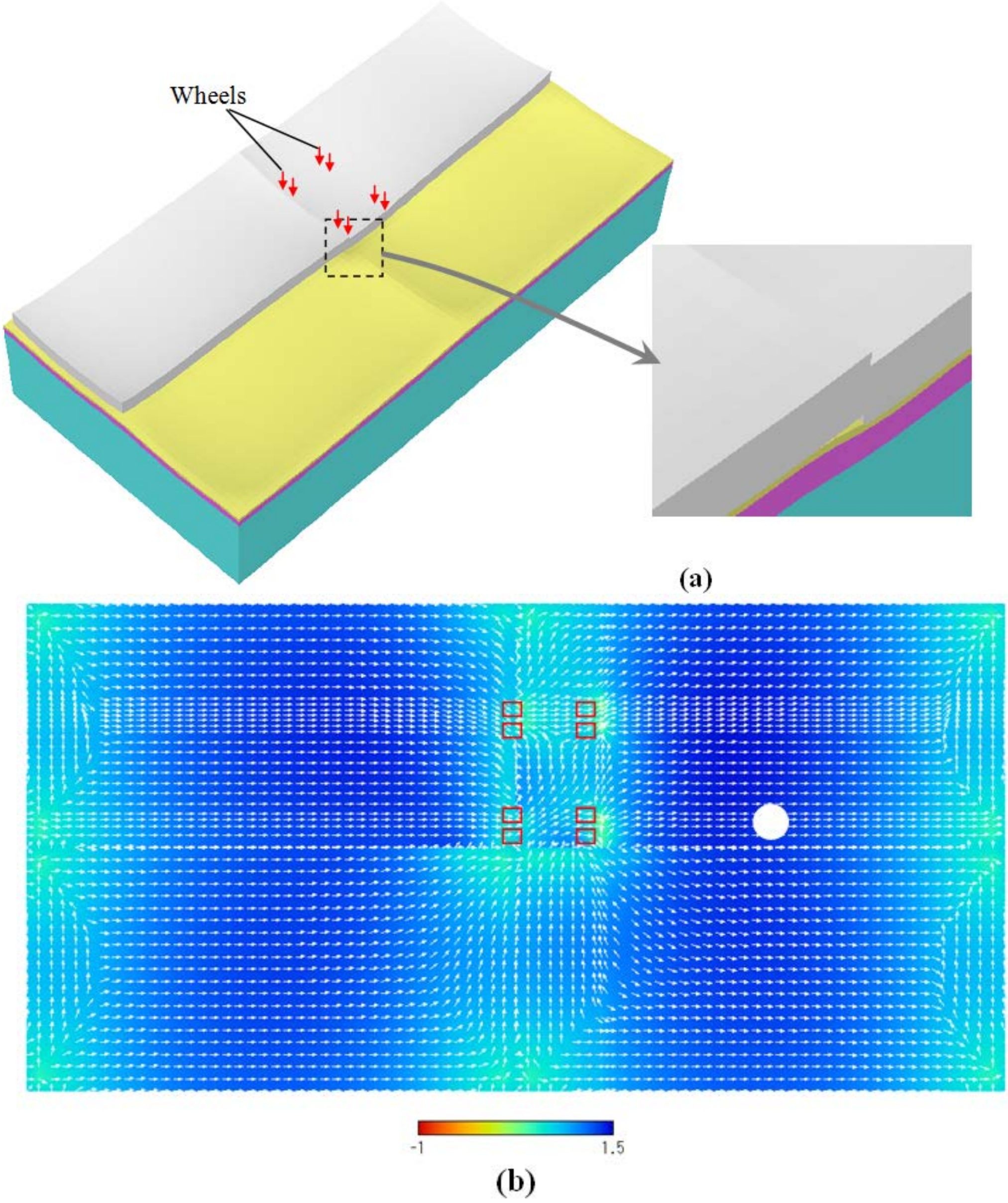

Figure 7. Deformations and top stress contour of road pavement: (a) curling deformation due to wheel and negative thermal loads, (b) contour and directions of the top maximum principal stress.

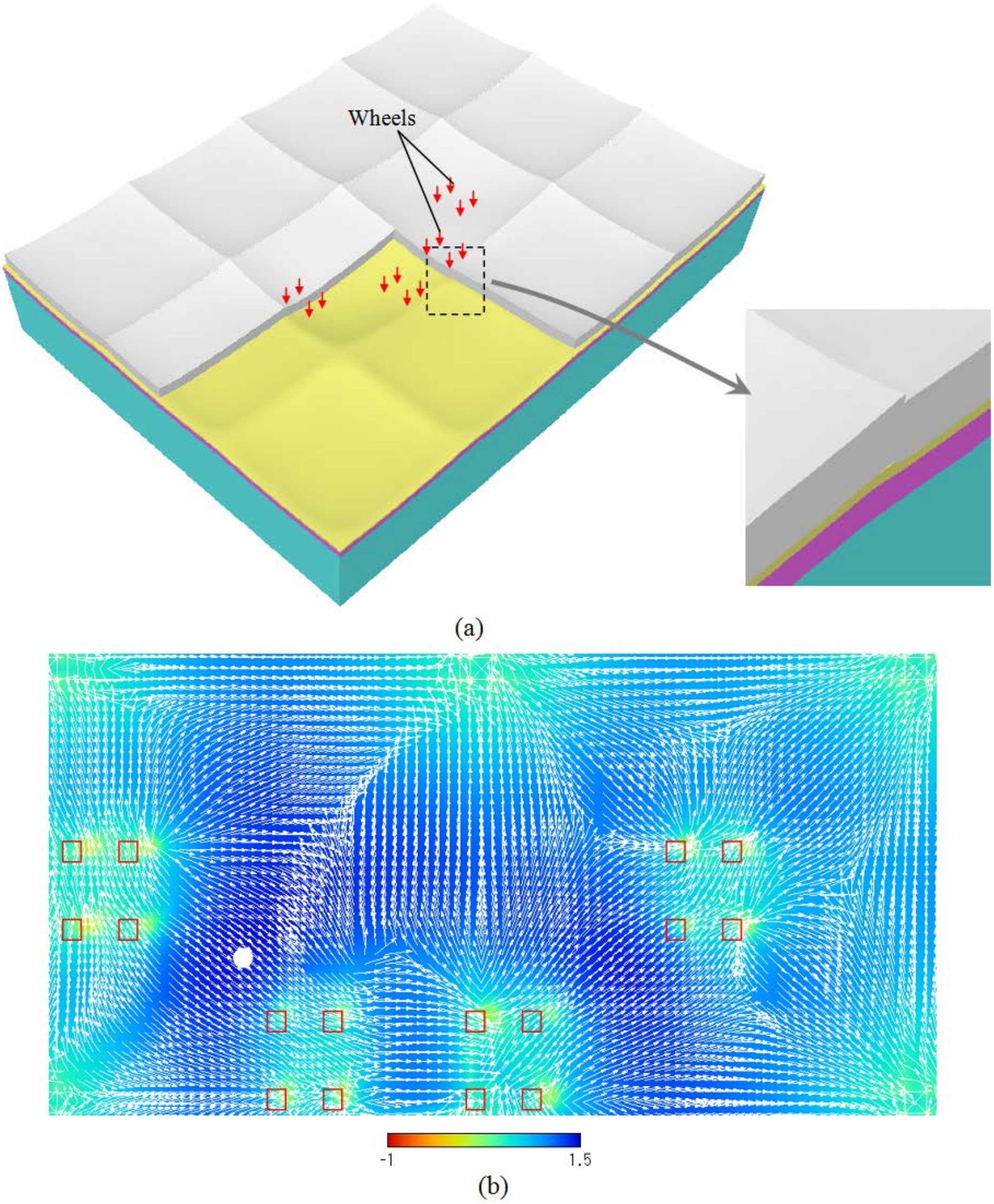

Figure 8. Deformations and top stress contour of airport pavement: (a) curling deformation due to wheel and negative thermal loads, (b) contour and directions of the top maximum principal stress.

Figure 8 shows the similar responses of the airport pavement. Loaded slabs largely deform downward and the underlying layer also deforms accordingly, as shown in Figure 8a. Therefore, no separation was observed in loaded areas. The contour of the top stress is much more complicated than the thermal stress. Large diagonal stresses appear in circular areas around the gears, which suggest the possibility of a corner cracking.

Maximum Combined Stresses. Table 3 summarizes the maximum combined stresses as well as the wheel and thermal stresses that were calculated separately at the same position. The maximum stress in the positive gradient appears at the bottom of the slab just under a wheel and that in the negative gradient appears at the top of the slab away from wheels as shown in Figures 7 and 8. A row of (a) in Table 3 presents the stresses when the wheel loads alone were applied and a row of (b) presents the stresses developed by the temperature gradient in the slab. The stresses in a row of (c) are the combined stresses produced by both wheel and thermal loads applied at the same time. The stresses in a row of (d) were obtained by simply adding stresses in the rows of (a) and (b). The difference between (c) and (d) is very small, less than 5 %. Therefore, simply adding wheel stress and thermal stress that are separately calculated is a reasonable way to estimate the combined stress. The bottom combined stresses are larger than the top stresses. In the 300mm thick slab, the ratio of the top combined stress to the bottom combined stress is 0.74. In the 460mm thick slab, it is 0.85. Therefore, the risk of surface cracking increases in the thicker slab.

Table 3. Maximum Combined Stresses (MPa).

Loading Condition	300mm		460mm	
	Negative(T)	Positive(B)	Negative(T)	Positive(B)
(a) Wheel Load	0.163	0.815	0.288	0.924
(b) Thermal Load	1.239	1.081	1.152	0.790
(c) Wheel & Thermal Loads	1.461	1.890	1.437	1.689
(d) = (a) + (b)	1.402	1.896	1.440	1.714

(T):on top surface, (B):on bottom surface

Effect of Doweled Joint. Dowel installation at joints is an effective way to reduce the combined stress. The effect of the dowels was investigated by comparing the combined stresses between doweled and non-doweled joints. Figure 9 compares stress distributions at the top of the slab between doweled and non-doweled joints in the road pavement. It can be seen that when dowels are used the maximum combined stress slightly decreases in the loaded slab, while the stress in the unloaded slab increases. Figure 10 shows similar comparisons in the airport pavement. The effect of dowel bar is more substantial in the airport pavement than that in the road pavement. It is because all joints in the airport pavement are doweled while the longitudinal joints in the road pavement are tied by a small diameter bars with a wide spacing.

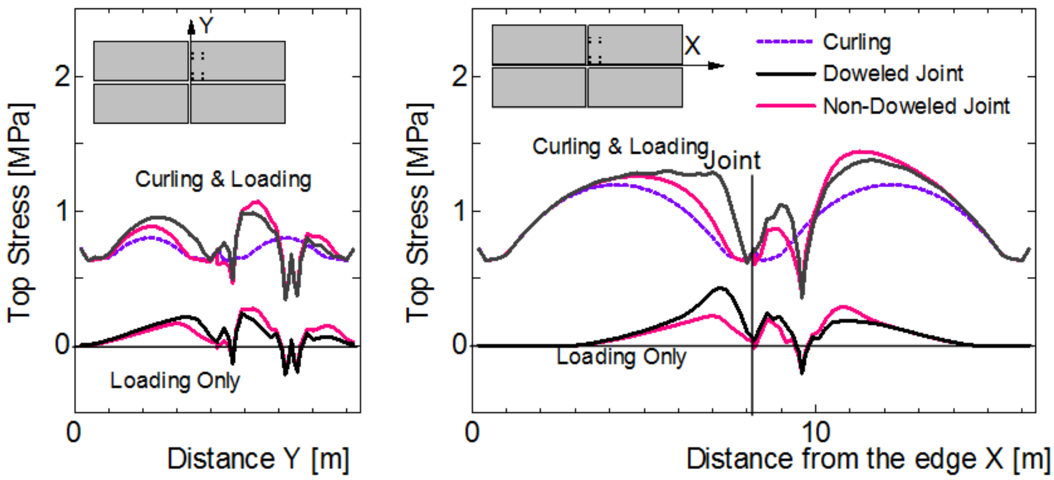

Figure 9. Comparison of stress distributions at the top of the slab between doweled and non-doweled joints in the road pavement.

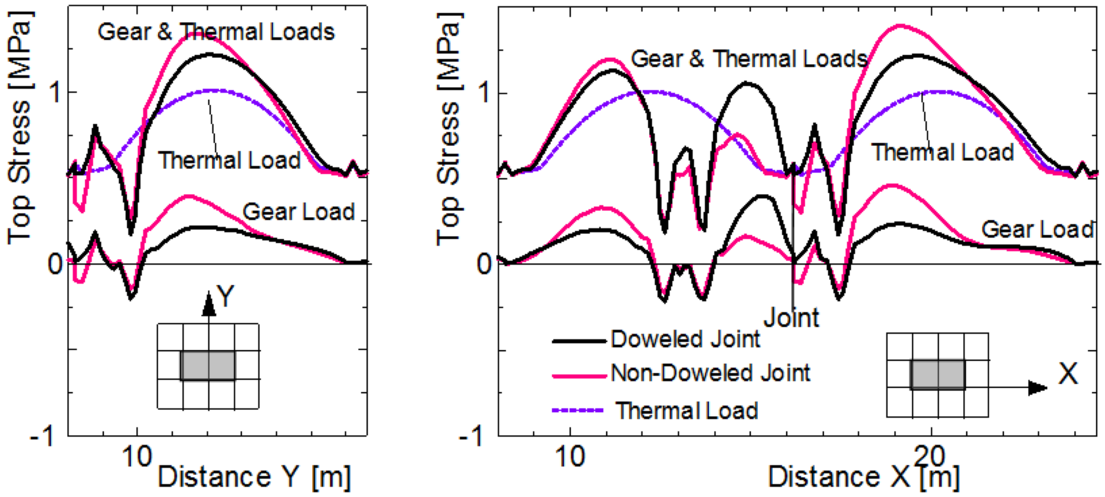

Figure 10. Comparison of stress distributions at the top of the slab between doweled and non-doweled joints in the airport pavement.

Conclusions

In this study, risk of top-down cracking in concrete pavement was investigated in terms of tensile stress on the top of concrete slabs due to wheel and negative thermal loads. 3DFEM simulations that took into account nonlinear temperature distributions throughout slab depth were performed to calculate the top tensile stresses on concrete pavements for a heavy duty road and an international airport. The following conclusions were drawn from this study:

1. Thermal stress analysis revealed that nonlinear negative temperature distribution produced relatively large tensile stress on the top of the slab, which cannot be precisely estimated by conventional thermal stress equations based on the linear temperature distribution.
2. Areas where the bottom surface of concrete slab was separated from the surface of underlying layer were small, because the underlying layer deformed similarly as the slabs deformed and the doweled joints restrain curling movement.
3. The maximum combined top stress occurred at a position away from the wheel loads. The ratio of the combined top stress in negative temperature gradient to the combined bottom stress in positive temperature gradient was greater in the airport pavement than that in the road pavement.
4. Simply adding wheel stress and thermal stress that are separately calculated is a reasonable way to estimate the combined stress.
5. The installation of dowels in joints is an effective measure to reduce the combined stress in loaded slabs.

References

ARA, Inc, ERES Consultants Division (2004). *Guide for Mechanistic-Empirical Design of New and Rehabilitated Pavement Structures*, National Cooperative Highway Research Program Project 1-37A.

Choubane, B. and Tia, M. (1995). “Analysis and Verification of Thermal-Gradient Effects on Concrete Pavement.” *J. Transportation Engineering*, ASCE, Vol.121, No.1, 1995.

Guo, E.H. (2005). “Fundamental Modeling of Curling Responses in Concrete Pavement.” *Proc. of 6th International DUT-Workshop on Fundamental Modeling of Design and Performance of Concrete Pavements,* (CD-ROM), Belgium.

Hiller, J.E., and Roesler, J.R. (2006). “Alternative Failure Modes for Long Life Jointed Plain Concrete Pavements.” *Proc., International Conference on Long-Life Concrete Pavements*, Chicago, Illinois, pp.265-283.

Iwama, S. (1963). “Experimental Studies on the Structural Design of Concrete Pavement.” JSCE.

Mahboub, K.C., Liu, Y., and Allen, D.L. (2004). “Evaluation of Temperature Responses in Concrete Pavement,” *J. Transportation Engineering*, ASCE, Vol.130, No.3, pp. 395-401.

Nishizawa, T., Koyanagwa, M., Takeuchi, Y., and Kimura, M. (2005). “Study on Mechanical Behavior of Dowel Bar in Transverse Joint of Concrete Pavement.” *Proc., 7th International Conference on Concrete Pavement*, Orland Florida, pp. 571-588.

Nishizawa, T., Ozeki, T., Katoh, K., and Matsui, K. (2009). “Finite Element Model Analysis of Thermal Stresses of Thick Airport Concrete Pavement Slabs.” *J. the Transportation Research Board*, No.2095, Transportation Research Board, pp. 3-12.

Pane, I., Hansen, W., and Mohamed, A.R. (1998). “Three-Dimensional Finite Element Study on Effects of Nonlinear Temperature Gradients in Concrete Pavements.” *Transportation Research Record*, No.1629, pp.58-65.

Shoukry, S.M., William, G.W., and Riad, M. (2003). “Nonlinear Temperature Gradient Effects in Dowel Jointed Concrete Slabs.” *Int. J. Pavement Engineering*, Vol.4, No.3, pp.131-142.